

Electronic Supplementary Information

Halide perovskite/lead sulfide heterostructure with enhanced photoelectrochemical performance for sensing of alkaline phosphatase (ALP)

Lei Deng^a, Fanghui Ma^a, Minghui Yang^{a*}, Xiaoqing Li^{b,c*}, Xiang Chen^{b,c*}

^a Hunan Provincial Key Laboratory of Micro & Nano Materials Interface Science, College of Chemistry and Chemical Engineering, Central South University, Changsha, China, 410083

^b Department of Dermatology, Xiangya Hospital, Central South University, Changsha, Hunan, China, 410000

^c National Engineering Research Center of Personalized Diagnostic and Therapeutic Technology, Central South University, Changsha, China, 410083

1. EXPERIMENTAL SECTION	Page S-2
1.1 Materials and Apparatus	Page S-2
1.2 Synthesis of CsPbBr₃ NCs and PbS	Page S-3
1.3 Preparation of GCE/CsPbBr₃ and GCE/CsPbBr₃/PbS	Page S-3
1.4 Construction of the PEC biosensor	Page S-4
2. Characterization	Page S-4
2.1 The morphology and microstructure	Page S-4
2.2 Characterization of the chemical valence states	Page S-6
3. Optimization of experimental conditions	Page S-8
4. Human serum sample analysis	Page S-9
Reference	Page S-10

1. EXPERIMENTAL SECTION

1.1 Materials and Apparatus.

Alkaline Phosphatase from bovine intestinal mucosa buffered aqueous solution (ALP, P6774-2KU), 1-octadecene (ODE, 90%), oleic acid (OA, 90%), oleylamine (OAm, 80-90%), phosphate buffered saline (PBS) and tris (hydroxymethyl) amino methane hydrochloride (Tris-HCl) were purchased from Sigma-Aldrich. Lead (II) bromide (PbBr_2 , 99.9%), cesium carbonate (Cs_2CO_3 , 99.9%), ethyl acetate ($\text{C}_4\text{H}_8\text{O}_2$, 99%) and sodium sulfide nonahydrate ($\text{Na}_2\text{S}\cdot 9\text{H}_2\text{O}$, 99.9%) were obtained from Macklin (Shanghai, China). Toluene (C_7H_8 , 99.5%) was bought from Sinopharm (Shanghai, China). Sodium thiophosphate (Na_3SPO_3 , 98%) was purchased from Bidepharm (Shanghai, China). Human serum samples were received from the Xiangya hospital (Changsha, China). All other reagents were of analytical grade and used without further purification. Ultrapure water (18.2 $\text{M}\Omega$ cm resistivity at 25°C, Milli-Q) was used in all experiments.

The transmission electron microscopy (TEM) images were obtained by JEOL JEM-2100 F electron microscopy. The micromorphology and energy-dispersive spectroscopy (EDS) were measured by scanning electron microscopy (FE-SEM, Hitachi S-4800). X-ray diffraction (XRD) characterization was conducted on X-ray diffractometer (XRD-7000, Shimadzu, Japan). The UV-visible diffuse reflectance spectra (DRS) were collected on a UV-vis spectrophotometer (Shimadzu, UV-2550). A 500 W Xe lamp with an emission wavelength of 420 nm was used as the light source and the light current was stable at 15.0 A. All PEC measurements were determined by electrochemical workstation (CHI 650D, China), which consists of a three-electrode system with custom made L-shaped glassy carbon electrode as working electrode (5 mm in diameter), Ag/AgCl electrode as reference electrode and platinum wire (Pt) as auxiliary electrode. Cyclic voltammetry (CV) and electrochemical impedance spectroscopy (EIS) were test in 0.1 M KCl containing 5.0 mM $\text{K}_4\text{Fe}(\text{CN})_6/\text{K}_3\text{Fe}(\text{CN})_6$ (1:1).

1.2 Synthesis of CsPbBr₃ NCs and PbS

The synthesis of CsPbBr₃ is a hot-inject method according to previous report with slight modification ¹. First, Cs-oleate was synthesized according to the following procedure: Cs₂CO₃ (0.407 g) was loaded into a 100 mL of 3-neck flask along with 1-octadecene (15 mL, ODE) and oleic acid (1.5 mL, OA). The mixture was evacuated for 20 min, dried for 1 h at 120°C, and then heated to 150°C under N₂ until all Cs₂CO₃ reacted with OA. Since Cs-oleate precipitates out of ODE at room-temperature, it has to be pre-heated to 100°C before injection.

Synthesis of CsPbBr₃ NCs: ODE (10 mL), PbBr₂ (0.138 g), OAm (1 mL) and OA (1 mL) were first transferred into a 100 mL three-necked flask with continuous stirring and dried under vacuum at 120°C for 30 min. The mixture was then heated in a N₂ atmosphere until PbBr₂ was completely dissolved, and the temperature was raised to 140°C before rapid injection of preheated Cs-oleate solution (1 mL). Afterwards, the mixture was cooled immediately by an ice-water bath. Finally, the aggregated nanocrystals were separated by centrifuging crude solution at 12000 rpm for 10 min under room temperature and washed by a mixed solvent of toluene (Tol) and ethyl acetate (EA) (Tol/EA = 1:1, v/v). Finally, the precipitate was re-dispersed in Tol (5 mL) and stored at 4 °C, aging for at least 5 days before use.

Synthesis of PbS: First, Na₂S solution (0.1 M) was prepared by dissolving Na₂S·9H₂O (0.969 g) in 40 mL ultrapure water. Then, 10 mL of the above solution was transferred into a 25 mL beaker and 1 mL of CsPbBr₃ toluene solution was added drop by drop under vigorous stirring for 10 min. The obtained PbS was then separated by centrifuging at 6000 rpm for 10 min, and the precipitate was washed with ethanol and water for three times and lyophilized overnight for use.

1.3 Preparation of GCE/CsPbBr₃ and GCE/CsPbBr₃/PbS

CsPbBr₃ film modified GCE (CsPbBr₃/GCE) was prepared by adding the above CsPbBr₃ with volume of 5 μL directly to the cleaned GCE surface and dried at room temperature. CsPbBr₃/PbS/GCE was fabricated after incubation 20 μL of 3 mM Na₂S solution with CsPbBr₃/GCE for 5 min. All modified electrode surfaces were thoroughly rinsed with Milli Q water and dried before carrying out electrochemical tests.

1.4. Construction of the PEC biosensor

To prepare the PEC sensor, 5 μL of CsPbBr_3 was dropped onto the surface of cleaned GCE. For ALP detection, 100 μL of 10 mM Tris-HCl (pH=8) containing 50 mM Na_3SPO_3 was mixed with 100 μL different concentrations of ALP and incubated for 8 h at 37°C . Then, 20 μL of reaction solution was dropped onto modified electrode surface and incubated for 5 min at room temperature, and then rinsed with Milli Q water to remove excess reactants. PEC assay was carried out in 10 mM PBS at a bias potential of -0.3 V.

2. Characterization

2.1 The morphology and microstructure

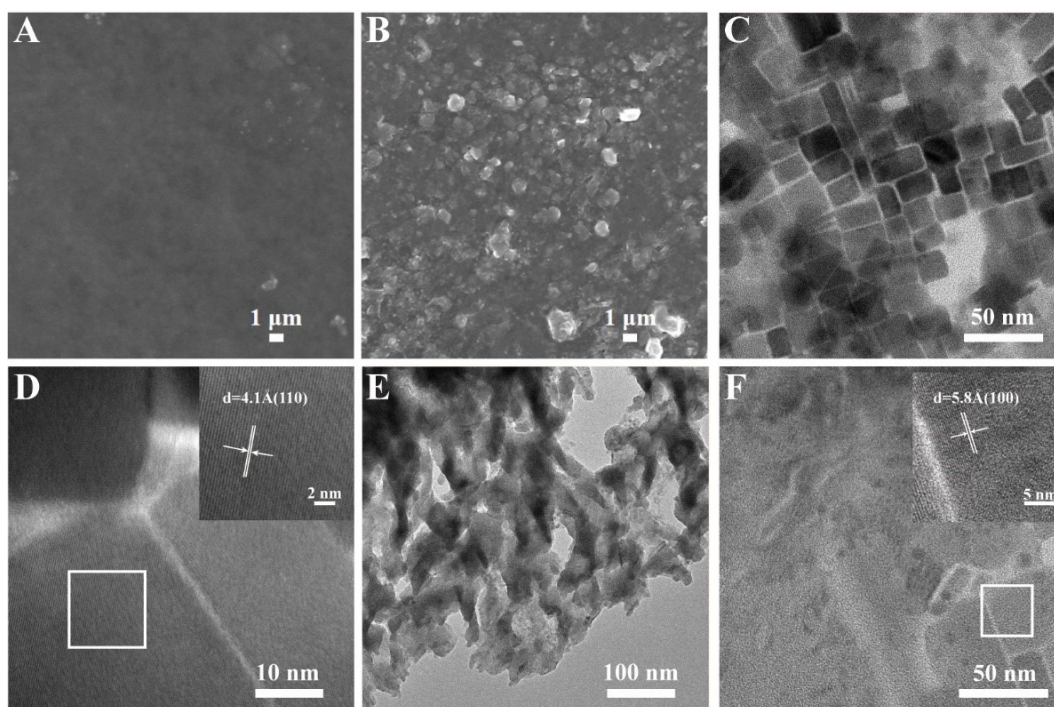


Figure S1. A. SEM image of CsPbBr_3 film; B. SEM image of $\text{CsPbBr}_3/\text{PbS}$ film; C. TEM image of CsPbBr_3 ; D. HRTEM image of CsPbBr_3 ; E. TEM image of PbS ; F. TEM image of $\text{CsPbBr}_3/\text{PbS}$.

The morphology and microstructure of the CsPbBr_3 and $\text{CsPbBr}_3/\text{PbS}$ modified electrodes were investigated by scanning electron microscopy (SEM) and transmission electron microscope (TEM). As shown in Fig. S1 A and B, a relatively dense film was formed on GCE by CsPbBr_3 , which attributes to the rapid volatilization of toluene solvent and abundance of organic ligands. When sulfur ions were added, the roughness of the modified electrode increased, which may lead to the increase of conductivity of

electrode surface, and that was consistent with the results of CV and EIS well. To further demonstrate the coexistence of PbS and CsPbBr₃, the composite film was tested using energy-dispersive spectroscopy (EDS) mapping in Fig. S2, which confirmed the uniform distribution of Cs, Pb, Br, S and C elements. TEM was employed to investigate the microstructure of CsPbBr₃ and CsPbBr₃/PbS. As shown in Fig. S1C, the diameters of CsPbBr₃ nanocrystals ranged from 15 ~ 30 nm. The lattice spacing was measured to be 0.41 Å which belongs to CsPbBr₃ lattice planes of (110) (Fig. S1D) ². For the synthesized PbS in Fig. S1E, the PbS was amorphous and it was difficult to observe the lattice. As shown in Fig. S1F, for CsPbBr₃/PbS composite, the cubic perovskite was coated with amorphous PbS, and the lattice fringe spacings is 0.58 Å, corresponding to the (100) crystal plane of CsPbBr₃ nanocrystals. These results displayed the morphology and microstructure of CsPbBr₃/PbS heterostructure.

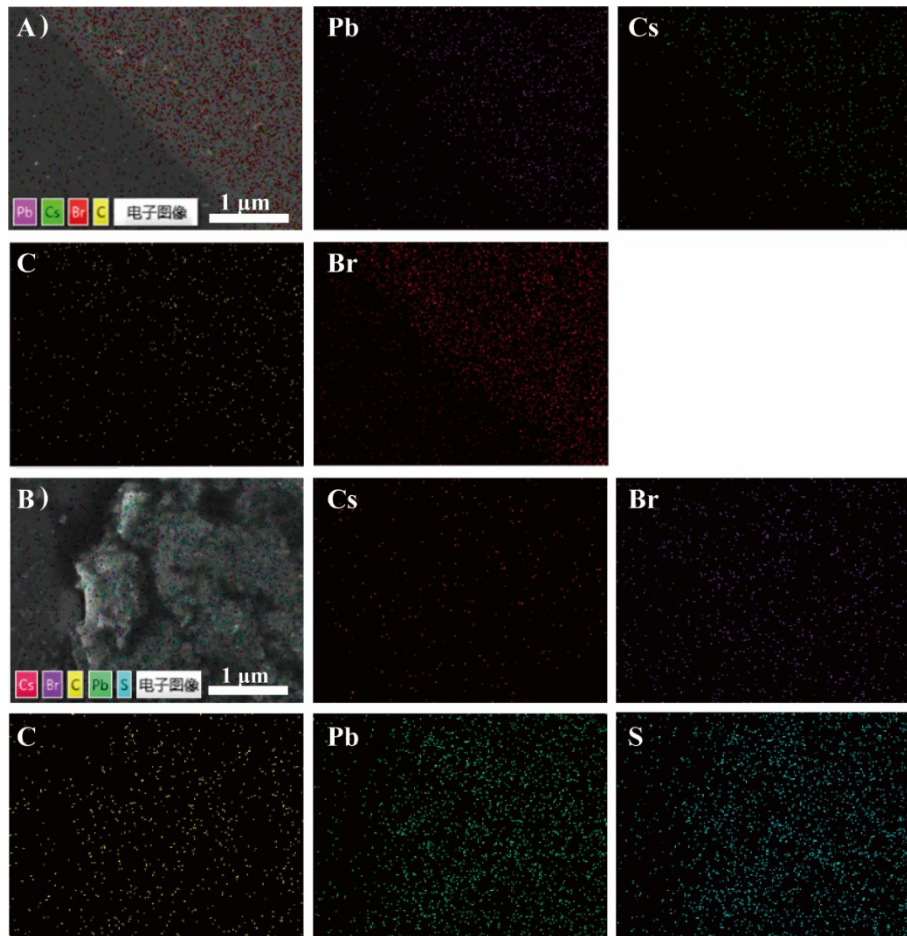


Figure S2. SEM image of CsPbBr₃ (A) and CsPbBr₃/PbS (B) with corresponding EDS mapping for Cs, Pb, Br, S and O elements.

2.2 Characterization of chemical valence states

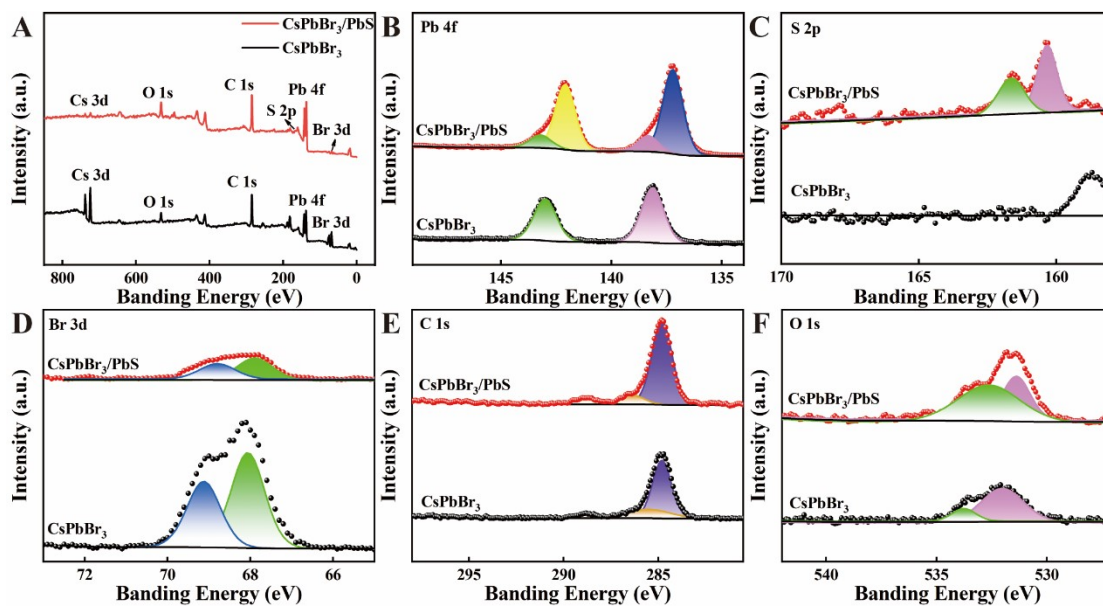


Figure S3. A. The survey scan XPS spectra of CsPbBr₃ and PbS; The element scans of Pb 4f (B), S 2p (C), Br 3d (D), C 1s (E), O 1s (F) spectra of CsPbBr₃ and PbS.

X-ray photoelectron spectroscopy (XPS) was used to compare chemical valence states of CsPbBr₃ samples before and after Na₂S treatment. Fig. S3A displays a survey scan XPS spectra of CsPbBr₃ and Na₂S treated CsPbBr₃ (CsPbBr₃/PbS), the characteristic peaks of Cs and Br were weak in CsPbBr₃/PbS sample, which indicates the surface of CsPbBr₃ were passivated. The high-resolution scans of Pb 4f spectra were shown in Fig. S3B. Both of CsPbBr₃ and CsPbBr₃/PbS appear to have a peak at 138.4 eV, which is assigned to the Pb-Br bond³, and the relative intensity of Pb-Br band decreased in CsPbBr₃/PbS. The peak at 137.2 eV in CsPbBr₃/PbS can be attributed to the Pb-S bond⁴, which certified the appearance of Pb-S band and the decrease of Pb-Br. The high-resolution scans of S 2p spectra were demonstrated in Fig. S3C, the characteristic peak of Pb-S observed at 161.2 eV present in CsPbBr₃/PbS and absent in CsPbBr₃. These results suggested that the Pb-S bond and Pb-Br bond existed in CsPbBr₃/PbS, which indicates the formation of CsPbBr₃/PbS heterojunctions. By the way, the peak at 158.5 eV in Fig. S3C belongs to Cs 4p,⁵ indicating that there was few Cs on the surface of CsPbBr₃/PbS sample. And the element scan of Br 3d spectra were shown in Fig. S3D, the weak characteristic peak of Br 3d in CsPbBr₃/PbS indicates that the content of Br element in CsPbBr₃/PbS is less than CsPbBr₃ sample. The peak of C

1s was corrected at 284.8 eV in Fig 3E. The characterization results of XPS proved that there was a large amount of Pb-S in CsPbBr₃/PbS samples, and confirmed the valence states of those elements in CsPbBr₃ and CsPbBr₃/PbS.

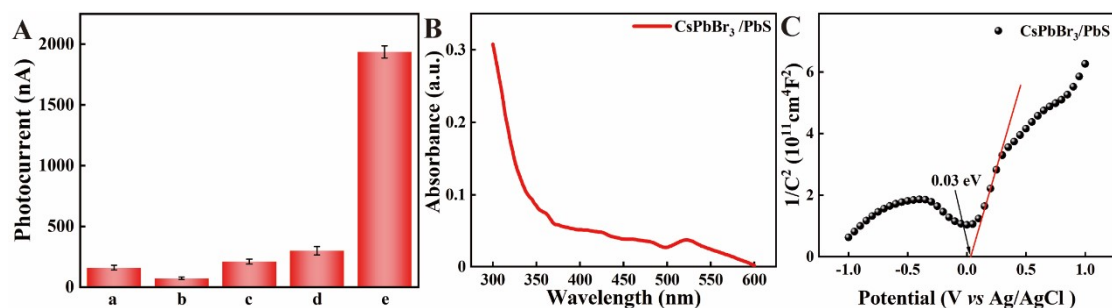


Figure S4 A. PEC responses of PbS (1 mg mL⁻¹) synthesized from Na₂S and different substances containing Pb element: a. Pb(CH₃COO)₂, b. PbO, c. PbBr₂, d. CsPb₂Br₅, e. CsPbBr₃; B. The UV-vis spectrum of CsPbBr₃/PbS; C. The Mott-Schottky plots of CsPbBr₃/PbS with 1000Hz.

The photocurrent responses of the black PbS synthesized from different substances containing Pb element with Na₂S were recorded. 1 mmol of Pb(CH₃COO)₂, PbO, PbBr₂ and CsPb₂Br₅ were mixed with 20 mL Na₂S solution (0.1M) respectively, and under ultrasonic reaction for 30 min, after wash and drying, the black PbS were synthesized. 1 mg mL⁻¹ PbS from Pb(CH₃COO)₂, PbO, PbBr₂, CsPb₂Br₅, CsPbBr₃ were add to GCE, and the photocurrent responses in 10 mM PBS at a bias potential of -0.3 V were recorded. As shown in Fig. S4A, the PbS synthesized by CsPbBr₃ NCs possessed excellent photocurrent response, other groups showed negligible photocurrent responses. The abundant ligands and special Pb arrangement on the surface of CsPbBr₃ NCs may be the reason for the enhanced photocurrent response.^{6, 7}

The UV-vis spectrum of CsPbBr₃/PbS was shown in Fig. S4B, the absorption band from 300 to 600 nm decreased, indicating that the light absorption of CsPbBr₃ was affected by PbS. And the Mott-Schottky plots of CsPbBr₃/PbS measured at a frequency of 1000Hz was shown in Fig. S4C, The E_{fb} of CsPbBr₃/PbS was 0.03 V vs Ag/AgCl, which was very close to the PbS's. This situation can be explained by PbS occupying the outermost surface site of the modified electrode. and maybe is the reason why the formation of heterojunction can improve the stability of perovskite structures in aqueous solution.

3. Optimization of experimental conditions

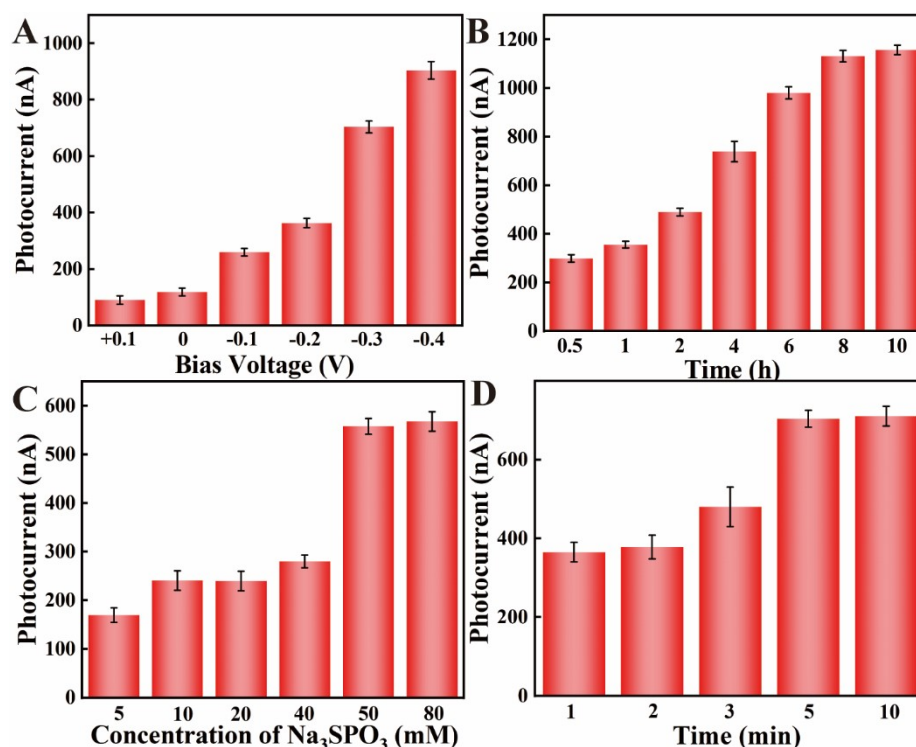


Figure S5 A. Optimized bias voltage; B. Optimized time of reaction of ALP and Na_3SPO_3 ; C. Optimized concentration of Na_3SPO_3 ; D. Optimized time of reaction on modified electrode.

Experimental conditions that affect the performance of the biosensor was studied.

The photocurrent intensity of GCE/ $\text{CsPbBr}_3/\text{PbS}$ under different bias voltages was illustrated in Fig. S5A. The photocurrent response of GCE/ $\text{CsPbBr}_3/\text{PbS}$ increased gradually with the change of the bias potential from 0.1 V to -0.4 V, but Pb(II) may deposit on the surface of electrodes on the bias potential of -0.4 V.^{8,9} Therefore, -0.3 V was chosen as the optimum bias potential for ALP detection. The incubation time of ALP with Na_3SPO_3 was also studied, and the photocurrent increased continuously until 8 h. As the catalytic substrate of ALP, the concentration of Na_3SPO_3 will also directly affect the amount of sulfur ions generated by enzymatic hydrolysis, and further affect the photocurrent response of the PEC sensor. As shown in Fig. S5C, the optimized concentration of Na_3SPO_3 was 50 mM. The optimal reaction time on modified electrode was 5 min.

4. Human serum sample analysis

Table S1. Determination of ATP in Human Serum Samples (n = 3) with the PEC biosensor

Spiked (U L ⁻¹)	Found (U L ⁻¹)	Recovery (%)	RSD (%)
100	107.2	107.2	4.3
200	206.1	103.5	4.2
300	272.9	91.1	2.4

Fresh human serum sample of healthy people was obtained from the Xiangya hospital (Changsha, China). 100 μ L 10 mM Tris-HCl containing 50 mM Na₃SPO₃ was mixed with 100 μ L human serum samples spiked with different concentration of ALP and incubated for 8 h at 37°C. Then, 20 μ L of reaction solution was dropped onto modified electrode surface and incubated for 5 min at room temperature. Finally, the electrode surface rinsed by Milli Q water before PEC measurements in 10 mM PBS at a bias potential of -0.3 V.

To assess the applicability of the PEC sensor, the sensor was used to determine ALP in human serum samples using a standard spiking method. The ALP level in normal people serum ranges from 40~100 U L⁻¹, but some people with cancer such as liver cancer, the ALP level in serum can be as high as 300 U mL⁻¹. Specific amounts of ALP (100, 200, 300 U L⁻¹) were added to the normal people serum and then analyzed. The recoveries were 107.2%, 103.5% and 91.1% with RSDs of 4.3%, 4.2% and 2.4%. Consequently, the results demonstrated that the PEC sensor may be used for analysis of ALP in human serum samples.

Reference

1. L. Protesescu, S. Yakunin, M. I. Bodnarchuk, F. Krieg, R. Caputo, C. H. Hendon, R. X. Yang, A. Walsh and M. V. Kovalenko, *Nano Lett.*, 2015, 15, 3692-3696.
2. Y. Jiang, J.-F. Liao, H.-Y. Chen, H.-H. Zhang, J.-Y. Li, X.-D. Wang and D.-B. Kuang, *Chem*, 2020, 6, 766-780.
3. Q. Y. Xiang, B. Z. Zhou, K. Cao, Y. W. Wen, Y. Li, Z. J. Wang, C. C. Jiang, B. Shan and R. Chen, *Chem. Mater.*, 2018, 30, 8486-8494.
4. M. M. R. Moayed, T. Bielewicz, H. Noei, A. Stierle and C. Klinke, *Adv. Funct. Mater.*, 2018, 28, 1706815.
5. B. V. Crist, *Handbook of Monochromatic XPS Spectra: The Elements of Native Oxides*, John Wiley & Sons, 2000.
6. C. F. Ma, C. W. Shi, K. Lv, C. Ying, S. S. Fan and Y. Yang, *Nanoscale*, 2019, 11, 8402-8407.
7. G. W. Hwang, D. Kim, J. M. Cordero, M. W. B. Wilson, C.-H. M. Chuang, J. C. Grossman and M. G. Bawendi, *Adv. Mater.*, 2015, 27, 4481-4486.
8. S. S. Li, M. Jiang, T. J. Jiang, J. H. Liu, Z. Guo and X. J. Huang, *J. Hazard. Mater.*, 2017, 338, 1-10.
9. L. A. Hutton, M. E. Newton, P. R. Unwin and J. V. Macpherson, *Anal. Chem.*, 2011, 83, 735-745.